

4.19

NEAR REAL-TIME SATELLITE CLOUD PRODUCTS FOR NOWCASTING APPLICATIONS

Patrick Minnis, Louis Nguyen, William Smith, Jr., John J. Murray
NASA Langley Research Center
Hampton, Virginia, USA

Rabindra Palikonda, Mandana Khaiyer, Douglas A. Spangenberg
AS&M, Inc.
Hampton, Virginia, USA

Patrick W. Heck
CIMSS, University of Wisconsin-Madison
Madison, Wisconsin, USA

Qing Z. Trepte
SAIC
Hampton, Virginia, USA

1. INTRODUCTION

Satellite imagery have been helpful in diagnosing certain meteorological conditions both subjectively and objectively in a nowcasting mode. However, such diagnoses are somewhat limited for automated usage because of a lack of quantification of the physical properties, especially those for clouds, observed in the imagery. With the continuous availability of well-calibrated research satellites and the advent of more spectral channels and higher resolution on geostationary satellite imagers such the GOES-I (Geostationary Operational Environmental Satellite) series or Meteosat Second Generation SEVIRI (Spinning Enhanced Visible InfraRed Imager), it has become possible to provide better quantification of cloud properties that are useful for diagnosing conditions such as aircraft icing potential and ceiling height or for providing other information such as surface radiation, cloud water content, or other parameters that would be useful for energy, agriculture, or weather forecast assimilation. This paper describes a set of cloud and radiation products that are now available within a few minutes of satellite

image times over much of North America and Europe and have the potential for a variety of applications.

Minnis et al. (2001) adapted algorithms used on low-Earth orbit satellite data for Earth radiation budget and cloud process studies to provide a variety of pixel-level products for the Atmospheric Radiation Measurement (ARM) Program over the central United States of America (USA) in near real-time. Smith et al. (2003) demonstrated that several of the derived products are useful for diagnosing aircraft icing potential. Because icing can occur anywhere, the products should not be limited the central USA. With the aid of the NASA Advanced Satellite Aviation-weather Products (ASAP) program, the ARM domain has recently been expanded to include the entire continental USA requiring the combination of 4-km data from both GOES East and West. This paper summarizes the current state of those products and their applicability to several now- and forecasting applications.

2. DATA & METHODOLOGY

The USA domain covers 25°N - 50°N and 65°W - 125°W, while the European domain currently stretches from 30°N to 55°N and 35°E to 12.5°W. Datasets used here include half-hourly GOES-10, and 12 4-km spectral radiances and the *Meteosat-8* 3-km

*Corresponding author address: Patrick Minnis, NASA Langley Research Center, MS 420, Hampton, VA 23681-2199. email: p.minnis@larc.nasa.gov.

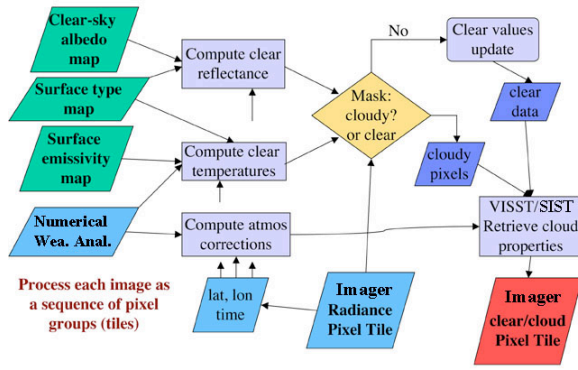


Fig. 1. Schematic real-time processing flow.

SEVIRI spectral radiances. GOES-10 at 135°W measures radiances at 0.65, 3.9, 10.8, and 12 μm GOES-12 at 75°W has the same configuration, except that the 12- μm channel was replaced with a 13.3- μm channel. GOES-12 data are analyzed over an area between 65°W and 105°W, while the GOES-10 data cover 90°W to 125°W. The results are stitched together at 99°W. SEVIRI channels corresponding to those on GOES-10 are used over the European domain.

Rapid Update Cycle (RUC) analyses (Benjamin et al., 2004) provide hourly profiles of temperature and humidity at a spatial resolution of 20 km. The 6-hourly NOAA Global Forecast Systems (GFS) analyses are used over Europe. The numerical weather analysis data are used to convert the retrieved cloud temperature T_c to cloud height z_c and correct radiances for atmospheric attenuation. Surface-type, clear-sky albedo, and surface emissivity maps are used to estimate the cloud-free radiances for a given scene as described by Minnis et al. (2001, 2004a).

The analysis procedure is outlined in Fig. 1, where the green boxes indicate relatively fixed input parameters and light blue denotes input that varies at each time step. The data are processed as tiles (1° region). After estimating the clear-sky radiances for each tile (gray boxes in center), each pixel is classified as clear or cloudy (tan box) based on a set of decision trees using three or four channels. If clear pixels are found in the tile, they replace the original clear radiance field for the tile and are used to derive the cloud properties for each cloudy pixel. For each clear pixel, the algorithm estimates surface skin temperature, the outgoing longwave radiation (OLR), and the clear-sky VIS and shortwave (ASW) albedos (not indicated in Fig. 1).

When the solar zenith angle SZA is less than 82° (daytime), cloudy pixels are analyzed with the visible infrared solar-infrared split-window technique (VISST; Minnis et al., 1995), which matches the observed values with theoretical models of cloud reflectance and emittance (Minnis et al. 1998). At night, and near twilight, cloudy pixels are detected as in Trepte et al. (2005) and the cloud properties are determined using the solar-infrared infrared split-window technique (SIST), an improved version of the 3-channel nighttime method of Minnis et al. (1995). It uses 3.9, 10.8, and 12.0- μm data for GOES-10 and SEVIRI, and only the first two channels for GOES-12. The methods estimate effective cloud temperature T_c , cloud height z and thickness h , phase, optical depth OD , effective droplet radius r_e or effective ice crystal diameter D_e , and LWP or ice water path IWP . Pixels with $T_c < 273$ K and identified as liquid water are designated as supercooled liquid (SLW) clouds. Other properties related to icing include h , OD , and LWP . Cloud thickness, used to find cloud base height, is estimated using the empirical parameterizations of Chakrapani et al. (2001). The top-of-atmosphere VIS albedo, ASW, and OLR are also computed for each cloudy pixel. The results are output for each tile (red box in Fig. 1).

Subsets of these results are then used to estimate the aircraft icing probability for each pixel in a tile and forwarded as input to evaluate icing severity in the Current Icing Potential (CIP) processing system (Politovich et al., 2004). The potential for aircraft icing depends on many factors related to the particular aircraft and the weather conditions. Some aircraft will accumulate ice in certain conditions while other planes will remain ice-free in the same cloud. These aircraft-related factors are not considered here. A necessary condition for icing is the presence of supercooled liquid water, relatively large droplets, and/or large concentrations of droplets or high liquid water content (LWC). SLW can be discriminated from warm clouds using T_c while the concentration of large droplets should be related to r_e . LWC can be estimated as the ratio of LWP/h . However, since both LWP and h depend on OD , only LWP is used here as a proxy for LWC. Smith et al. (2003) found some weak positive dependencies of icing intensity on LWP and r_e , and a weak negative dependency on T_c using matched VISST and in situ aircraft data.

Minnis et al. (2004b) developed a probability based method to classify the icing potential for each pixel based on pilot reports (PIREPS). Any pixels classified as cloudy with $T_c > 272$ K, as clear, or as an ice cloud with $OD < 6$ are considered as icing potential candidates. Ice clouds with $OD > 6$ are considered as indeterminate pixels because the nature of any clouds below the ice cloud currently cannot be discerned. Icing probability for remaining pixels is estimated as

$$IP = 0.147 \ln(LWP) - 0.084, \quad (1)$$

for $r_e = 5 \mu\text{m}$, and

$$IP = 0.138 \ln(LWP) - 0.024, \quad (2)$$

for $r_e = 16 \mu\text{m}$. Linear interpolation between the results of (1) and (2) are used for pixels with r_e between 5 and 16 μm . Pixels with larger or smaller values of r_e are assigned the appropriate extreme value. Low, medium, and high probabilities correspond to $IP < 0.4$, $0.4 \leq IP < 0.7$, $IP \geq 0.7$, respectively. The intensity of icing is classified as light or moderate-severe if LWP is less or greater than 432 gm^{-2} , respectively. This approach to estimating the probability for icing is considered as a preliminary technique because it is based on only 11 days of PIREPS and GOES-12 data taken during February 2004. As reported later, Minnis et al. (2001c) evaluated it using an additional 18 and 11 days of GOES-12 and 10 data, respectively.

3. RESULTS

Figure 2 shows an example of the USA results for GOES-10/12 imagery taken at 1645 UTC, 6 May 2005. The pseudocolor RGB image (Fig. 2a) reveals the various cloud types in a single image. In this type of image, red is assigned to the visible reflectance, the temperature difference between the 3.9 and 11- μm channels determines the green intensity, and the 11- μm temperature T provides the blue intensity on an inverse scale. Snow-free clear areas, like much of the northwestern Mexico, are green, blue, or tan while clear snow-covered areas such as northern Quebec are typically bright or dark pink. High clouds are generally bluish white or gray (e.g., Colorado, north central Mexico) or some shade of magenta (e.g., western USA and over the Atlantic), while low or midlevel clouds are often white (e.g., Great Lakes) or

a shade of peach or orange (e.g., Florida and Pacific). The retrieved cloud phase image (Fig. 2b) shows clear areas in green, warm liquid water clouds in dark blue, SLW clouds in light blue, and ice clouds in red. The edges of some ice clouds are classified as warm water because of the weak signals emanating from the partially cloud-filled pixels. SLW clouds are seen over the Great Lakes area, the northwestern USA, and near the large storm over the east coast. Other SLW clouds are false returns due to thin cirrus clouds over warm water clouds (e.g., north central Mexico, Nebraska). Low clouds ($z < 3$ km) are common over many areas (Fig. 2c) with bases often below 1 km (Fig. 2d). The derived values of r_e (Fig. 2c) are typically between 7 and 11 μm but greater values occur off the California coast and over southeastern USA. In some overlapped conditions along the edges of ice clouds (e.g., north central Mexico) or for relatively thin clouds over snow (Quebec), the VISST often retrieves a large value of r_e because the 3.9- μm radiance is diminished due to absorption by ice in the form of large cirrus crystals or snow grains. Optical depths for ice clouds that are not attached to storm systems are typically less than 4 (Fig. 2f) but are much larger in the developed large-scale disturbances. Low-cloud optical depths are also quite variable. The cloud LWP (Fig. 2g) reaches extremely high values, exceeding 400 gm^{-2} , around Lake Superior and off the Georgia coast. More commonly, LWP is less than 150 gm^{-2} . Severe icing is detectable only in a few locations such as the Great Lakes, mid-Atlantic coast, and in Oregon (Fig. 2h). Probabilities for light icing are more common. In some instances, the light icing is designation is incorrect (e.g., Mexico) because of the overlapped cloud effects noted above. Icing conditions may be present in other areas, but cannot be detected because of the overlying thick ice clouds (white). The speckling results from cloud edge effects. The vertical extent of the potential icing clouds can be estimated from the cloud-top and base altitudes of the clouds.

Figure 3 shows a smaller subset of retrievals for the European domain derived from a SEVIRI image taken at 0800 UTC, 2 May 2005. The clear desert shows up as tan regions in the RGB image, while clear water and other land types are typically dark green (Fig. 3a). Low clouds are seen over eastern Europe, north of Algeria and behind the frontal system

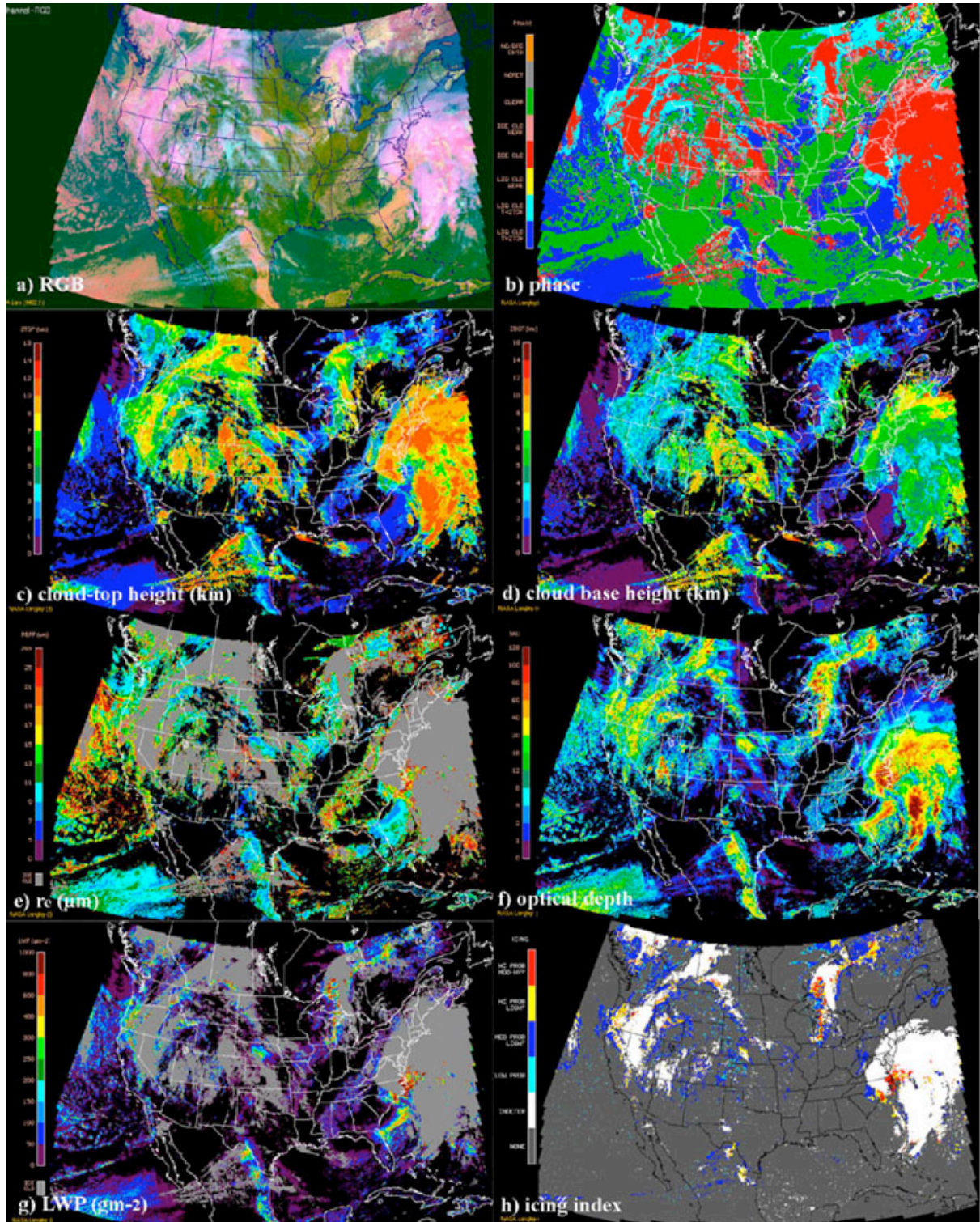


Fig. 2. Selected cloud and aircraft icing parameters from GOES-10 and 12, 1645 UTC, 6 May 2005. Gray indicates ice clouds in (e) and (g) and no icing in (h). Color bar ranges: (b) warm clouds - dark blue and yellow, SLW - light blue, ice clouds - red or pink; (c & d) 0 - 8 km (purple - yellow), 8 - 16 km (orange - deep red); (e) 5 (blue) to 21 μm (dark orange), > 21 μm , reds; (f) \log_2 0 - 8 (purple - light blue), 8 - 20 (greens), 20 - 100 (yellow - bright red), > 100 - deep red (g) 0-300 gm^{-2} , purple - light green; 300 - 400 gm^{-2} , yellow; 400 - 1000 gm^{-2} , orange to dark red; (h) low probability - light blue, medium probability of light icing - dark blue, high probability of light icing - yellow, high probability of medium to severe icing - red, indeterminate - white.

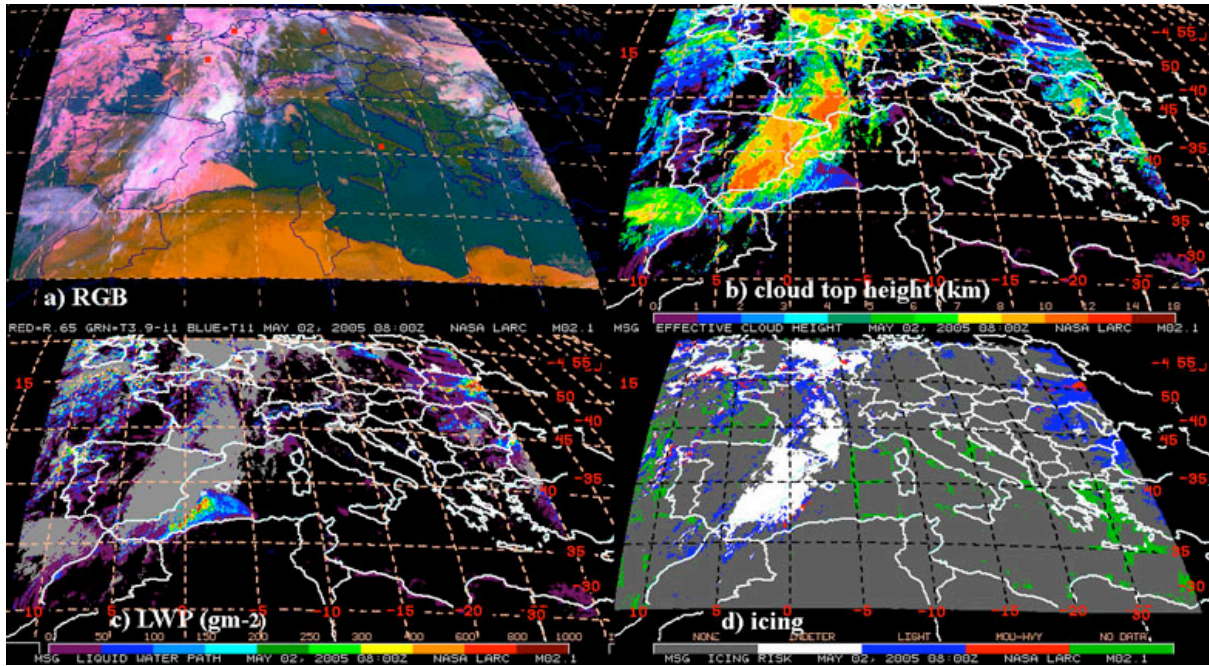


Fig. 3. Selected cloud and aircraft icing parameters from Meteosat-8 SEVIRI, 0800 UTC, 2 May 2005. Color bar ranges: (b) 0 – 8 km (purple – yellow), 8 – 16 km (orange – deep red); (c) 0–300 gm^{-2} (purple to light green), 300 – 400 gm^{-2} (yellow), 400 – 1000 gm^{-2} (orange to dark red); (g) no icing – green and gray; light – blue, medium to severe – red, indeterminate – white.

that extends from the North Sea through Spain (Fig. 3b). Large values of LWP occur over the Mediterranean and Ukraine (Fig. 3c). Most values of LWP, however, are less than 50 gm^{-2} . Severe icing conditions are diagnosed only over western Ukraine and along the edges of ice clouds behind the front.

The cloud property and icing methodologies are currently being applied in near-real time to GOES-10 and 12 data every half hour during the daytime and hourly at night. The results from each satellite are available separately and stitched together. The Meteosat-8 retrievals are performed each hour. All of the data can be accessed digitally or in image form at www-angler.larc.nasa.gov/satimage/products.

4. DISCUSSION

The example results presented above serve as samples of the products currently being generated, but the algorithms used to derive each product are continually being updated as validation studies provide new information or advanced methods become available. Validation efforts have demonstrated that properties like cloud fraction, base height, optical depth, particle size, and ice and liquid water path (e.g., Dong et al., 2002; Min et al., 2004; Khaiyer et al. 2005; Doelling et al. 2005) are reasonably well correlated

with and similar in magnitude to in situ and active remote sensing retrievals. In situ data from a variety of field measurements as well as PIREPS have been used to validate the satellite icing measurements (e.g., Smith et al., 2003; Minnis et al., 2004b; Nguyen et al., 2004). From more recent in situ data, Haggerty et al. (2005) demonstrated that the LWP and r_e retrievals are related to icing severity and should be a valuable addition to the CIP nowcasting product. Other validation efforts are underway.

In a comparison of PIREPS with results from an earlier version of the GOES products, Minnis et al. (2004c) found that the algorithm missed icing conditions in 5% of the cases indicated as icing by PIREPS and produced false icing in 15% of the cases. Of the 31% of the cases classified as indeterminate, the PIREPS indicated that icing occurred 70% of the time. Thus, when it could determine icing or not (all cases that were not indeterminate), the algorithm matched the PIREPS in 73% of the cases, but still missed nearly 50% of the icing cases, primarily due to the indeterminate conditions.

Many of the false negatives result from relatively small LWP values and may be affected by the time differences between the satellite image and the PIREP report location. The false positives are likely due to spatial-temporal mismatch, the use of probability

estimates, and, in many instances, the overlapping cloud effects that cause the false SLW classifications noted earlier. The largest mismatches, however, are due to the indeterminate conditions.

The indeterminate errors can be minimized directly or indirectly. The indirect method, which is currently being implemented, is to blend the results with the CIP and use the cloud products primarily for assessing the severity of the icing potential (e.g., Haggerty et al., 2005). The direct approach would utilize algorithm enhancements and blending of other data into the satellite analysis stream and would eliminate many of the false positives while reducing the indeterminate cases. Multilayer cloud detection algorithms can be used to determine when a thin cirrus overlies a thick water cloud (Minnis et al., 2005a). The temperature of the low-level clouds can be estimated using data from nearby low clouds and the presence or absence of SLW can be determined in those cases. That procedure should eliminate many of the false positives and significantly reduce the number of indeterminate cases.

Remaining indeterminate pixels correspond to clouds with an optically thick cirrus above or to a deep convective cloud that is water on the bottom and ice on top. The icing conditions for many of these remaining cases could be resolved by incorporating data from other sources (Minnis et al., 2005a). For example, cloud bases measured with the Automated Surface Observing System (ASOS) ceilometers can be used to determine if a low cloud deck is present under the ice clouds. Based on the properties of low clouds in the surrounding areas, it would be possible to estimate the icing potential for the indeterminate pixels when the cloud base is too high relative to the ASOS measurements. If the satellite and ASOS cloud base heights agree to within some tolerance, then the indeterminate pixel could be classified. If the ASOS base is significantly lower, then the properties of nearby low clouds could be assigned to those pixels.

To provide more continuous coverage, numerical weather analysis (NWA) or forecast data could be used in a similar fashion using relationships between the model relative humidities and actual cloud cover (e.g., Minnis et al., 2005b). The comprehensive direct approach would fill out the satellite data in the vertical using multilayered detection methods, ceilometer cloud

base estimates, and NWA data. This technique for developing a 3-D dataset needs further exploration.

4. CONCLUDING REMARKS

A new, physically based method for real-time estimation of the probability of icing conditions during daytime has been developed for use with newer geostationary satellite imagery. The algorithm produces pixel-level cloud and radiation properties as well as an estimate of icing probability with an associated intensity rating. Because icing depends on so many different variables, such as aircraft size or air speed, it is not possible to achieve 100% success with this or any other type of approach. This initial algorithm, however, shows great promise for diagnosing aircraft icing and putting it at the correct altitude within 0.5 km most of the time (Minnis et al. 2004c). Although it is being incorporated into the CIP, additional research should be conducted to make it more reliable as input for the operational CIP and as a stand-alone nowcasting product. The delineation of the icing layer vertical boundaries will need to be improved using either the NWA or balloon soundings or ceilometer data to adjust the cloud base height, a change that would require adjustment of the cloud-top altitude also.

Only daytime data have been considered so far. While the SIST has demonstrated some skill in discriminating between optically thin and thick clouds at night, the utility of the resulting products for icing classification has not yet been examined. Most of the indeterminate daytime cases were found to be a combination of a high ice clouds over an icing cloud. Better detection of multilayered clouds and blending of ceilometer data and NWA soundings could be used to diagnose clouds underneath the satellite-observed cirrus clouds. Similar methods are already being used to develop the current CIP product and could be adapted to work in a conditional probability scenario with the satellite retrievals. False returns caused by thin cirrus clouds over warm, low cloud decks can also be minimized by using the multispectral IR methods to detect thin cirrus clouds. Such techniques typically rely on the 12- μm data, which are currently not available GOES-12. Hopefully, future GOES imagers will return the 13.3- μm channel on GOES-12 to the original 12- μm channel.

The satellite icing algorithms are just one part of a comprehensive aircraft icing program being developed by NASA, NOAA, and the FAA. Ultimately, the results will be combined with PIREPS, model forecasts, and other data within the CIP to provide a near-real time optimized characterization of icing conditions for pilots and flight controllers. The cloud products have a number of other potential uses including assimilation into weather forecast models, ceiling estimates, and for energy applications. Future versions of the VISST output will include estimates of the surface skin temperature, the surface radiation budget (Nordeen et al., 2005) and cloud layering (Minnis et al., 2005a).

ACKNOWLEDGEMENTS

This research was supported by the NASA Aviation Safety Program through the NASA Advanced Satellite Aviation-weather Products Initiative and by the NASA Radiation Sciences Program.

REFERENCES

- Benjamin, S. G., D. Dévényi, S. S. Weygandt, K. J. Brundage, J. M. Brown, G. A. Grell, D. Kim, B. E. Schwartz, T. G. Smirnova, and T. L. Smith, and G. S. Manikin, 2004: An hourly assimilation-forecast cycle - the RUC. *Mon. Wea. Rev.*, **132**, 495-518.
- Chakrapani, V., D. R. Doelling, A. D. Rapp, and P. Minnis, 2002: Cloud thickness estimation from GOES-8 satellite data over the ARM SGP site. *Proc. 12th ARM Science Team Mtg*, April 8-12, St. Petersburg, FL, 14 pp. (Available, www.arm.gov/docs/documents/technical/conf_0204/chakrapani-v.pdf)
- Doelling, D. R., D. Phan, D. A. Spangenberg, and P. Minnis, 2005: Validation of retrieved cloud amounts over the continental US with ASOS ceilometer data. *Proc. 15th ARM Sci. Team Mtg.*, Daytona Beach, FL, March 14-18. (Available at www.arm.gov/publications/proceedings/conf15/extended_abs/doelling_dr.pdf)
- Dong, X., P. Minnis, G. G. Mace, W. L. Smith, Jr., M. Poellot, R. T. Marchand, and A. D. Rapp, 2002: Comparison of stratus cloud properties deduced from surface, GOES, and aircraft data during the March 2000 ARM Cloud IOP. *J. Atmos. Sci.*, **59**, 3256-3284.
- Haggerty, J., G. Cunning, B. Bernstein, P. Minnis, and R. Palikonda, 2005: Integration of advanced satellite products into an icing nowcast system. *Proc. WWRP Symp. Nowcasting & Very Short Range Forecasting*. Toulouse, France, 5-9 September, 4.14.
- Khaiyer, M., R. Arduini, P. Minnis, J. Huang, R. Palikonda, G. Nowicki, and B. Lin, 2005: Comparisons of cloud liquid water paths over the ARM SGP using satellite and surface data: validation of new models. *Proc. 15th ARM Sci. Team Mtg.*, Daytona Beach, FL, March 14-18. (Available, www.arm.gov/publications/proceedings/conf15/extended_abs/khaiyer_mm.pdf)
- Min, Q, P. Minnis, and M. M. Khaiyer, 2004: Comparison of cirrus optical depths from GOES-8 and surface measurements. *J. Geophys. Res.*, **109**, D15, D15207 10.1029/2003JD004390.
- Minnis, P., D. P. Garber, D. F. Young, R. F. Arduini, and Y. Takano, 1998: Parameterization of reflectance and effective emittance for satellite remote sensing of cloud properties. *J. Atmos. Sci.*, **55**, 3313-3339.
- Minnis, P., et al., 1995: Cloud Optical Property Retrieval (Subsystem 4.3). "Clouds and the Earth's Radiant Energy System (CERES) Algorithm Theoretical Basis Document, Volume III: Cloud Analyses and Radiance Inversions (Subsystem 4)", *NASA RP 1376 Vol. 3*, pp. 135-176.
- Minnis, P., W. L. Smith, Jr., L. Nguyen, M. M. Khaiyer, D. A. Spangenberg, P. W. Heck, R. Palikonda, B. C. Bernstein, and F. McDonough, 2004b: A real-time satellite-based icing detection system. *Proc. 14th Intl. Conf. Clouds and Precipitation*, Bologna, Italy, 18-23 July.
- Minnis, P., Y. Yi, J. Huang, and J. K. Ayers, 2005a: Relationships between meteorological conditions and cloud occurrence determined from ARM data. Accepted, *J. Geophys. Res.*, 10.1029/2005JD006005.
- Minnis, P., M. Khaiyer, Y. Yi, S. Sun-Mack, R. Palikonda, D. Spangenberg, and J. Huang, 2005b: Developing a 3-D cloud product over the ARM sites using GOES data. *Proc. 15th ARM Sci. Team Mtg.*, Daytona Beach, FL, March 14-18. (Available, www.arm.gov/publications/proceedings/conf15/extended_abs/minnis_p.pdf)

- Minnis, P., L. Nguyen, W. L. Smith, Jr., M. M. Khaiyer, R. Palikonda, D. A. Spangenberg, D. R. Doelling, D. Phan, G. D. Nowicki, P. W. Heck, and C. Wolff, 2004c: Real-time cloud, radiation, and aircraft icing parameters from GOES over the USA. *Proc. 13th AMS Conf. Satellite Oceanogr. and Meteorol.*, Norfolk, VA, Sept. 20-24, CD-ROM, P7.1.
- Minnis, P., W. L. Smith, Jr., D. F. Young, L. Nguyen, A. D. Rapp, P. W. Heck, S. Sun-Mack, Q. Trepte, and Y. Chen, 2001: A near-real time method for deriving cloud and radiation properties from satellites for weather and climate studies. *Proc. AMS 11th Conf. Satellite Meteorology and Oceanography*, Madison, WI, Oct. 15-18, 477-480.
- Minnis, P., D. F. Young, S. Sun-Mack, Q. Z. Trepte, R. R. Brown, S. Gibson, and P. Heck, 2004a: Diurnal, seasonal, and interannual variations of cloud properties derived for CERES from imager data. *Proc. 13th AMS Conf. Satellite Oceanogr. and Meteorol.*, Norfolk, VA, Sept. 20-24, CD-ROM, P6.10.
- Nordeen, M. L., M. M. Khaiyer, D. R. Doelling, and D. N. Phan, 2005: Comparison of surface and satellite-derived cloud and radiation properties at the Atmospheric Radiation Measurement Southern Great Plains and Tropical Western Pacific sites. *Proc. 15th ARM Sci. Team Mtg.*, Daytona Beach, FL, March 14-18. (Available http://www.arm.gov/publications/proceedings/conf15/extended_abs/nordeen_ml.pdf)
- Nguyen, L., P. Minnis, D. A. Spangenberg, M. L. Nordeen, R. Palikonda, M. M. Khaiyer, and I. Gultepe, 2004: Comparison of satellite and aircraft measurements of cloud microphysical properties in icing conditions during ATREC/AIRS-II. *Proc. AMS 11th Conf Aviation, Range, and Aerospace*. Hyannis, MA, October 4-8, CD-ROM, P6.10.
- Politovich, M. K., F. McDonough, and B. C. Bernstein, 2004: The CIP in-flight icing severity algorithm. *Proc. AMS 11th Conf Aviation, Range, and Aerospace*. Hyannis, MA, October 4-8, CD-ROM, P6.3.
- Smith, W. L., Jr., P. Minnis, B. C. Bernstein, F. McDonough, and M. M. Khaiyer, 2003: Comparison of supercooled liquid water cloud properties derived from satellite and aircraft measurements. *Proc. FAA In-Flight Icing/De-icing International Conference*, Chicago, IL, June 16-20, CD-ROM, 2003-01-2156.
- Trepte, Q. Z., P. Minnis, and R. Palikonda, 2005: Improvements in near-terminator and nocturnal cloud masks using satellite imager data over the ARM sites. *15th ARM Sci. Team Mtg.*, Daytona Beach, FL, March 14-18. (Available at http://www.arm.gov/publications/proceedings/conf15/extended_abs/trepte_qz.pdf)